Wildfire smoke injection heights: Two perspectives from space

Ralph A. Kahn,[1,2] Yang Chen,[1] David L. Nelson,[3] Fok-Yan Leung,[4] Qinbin Li,[1] David J. Diner,[1] and Jennifer A. Logan[4]

Received 27 September 2007; revised 5 December 2007; accepted 18 January 2008; published 22 February 2008.

[1] The elevation at which wildfire smoke is injected into the atmosphere has a strong influence on how the smoke is dispersed, and is a key input to aerosol transport models. Aerosol layer height is derived with great precision from space-borne lidar, but horizontal sampling is very poor on a global basis. Aerosol height derived from space-borne stereo imaging is limited to source plumes having discernable features. But coverage is vastly greater, and captures the cores of major fires, where buoyancy can be sufficient to lift smoke above the near-surface boundary layer. Initial assessment of smoke injection from the Alaska-Yukon region during summer 2004 finds at least about 10% of wildfire smoke plumes reached the free troposphere. Modeling of smoke environmental impacts can benefit from the combined strengths of the stereo and lidar observations.
Citation: Kahn, R. A., Y. Chen, D. L. Nelson, F.-Y. Leung, Q. Li, D. J. Diner, and J. A. Logan (2008), Wildfire smoke injection heights: Two perspectives from space, *Geophys. Res. Lett.*, *35*, L04809, doi:10.1029/2007GL032165.

[2] Smoke injection heights are key inputs for aerosol transport modeling, as they are critical for determining the distance and direction the smoke will travel [e.g., *Westphal and Toon*, 1991; *Ginoux et al.*, 2001; *Colarco et al.*, 2004]. A recent paper in the *Journal of Geophysical Research, Atmospheres* analyzed the injection heights of wildfire smoke and other aerosol plumes near their sources, using stereo-derived plume heights from the Multi-angle Imaging SpectroRadiometer (MISR) that flies aboard the NASA Earth Observing System's Terra satellite [*Kahn et al.*, 2007]. This study reported smoke from major wildfires injected into layers of relative stability above the atmospheric boundary layer (ABL) in the immediate vicinity of the sources themselves. It concluded that the buoyancy generated by the fires studied could account for these observations, within the limitations of a crude plume entrainment model, and the uncertainty of assumed fire radiant emissivity. However, the analysis, as well as previous studies of individual wildfire plumes [e.g., *Fromm and Servranckx*, 2003], made no attempt at characterizing the frequency with which above-boundary-layer injection occurs on a regional or global basis.

[3] An independent investigation of smoke aerosol height, performed using data from the Cloud-Aerosol Lidar with Orthogonal Polarization (CALIOP) that flies aboard the joint US (NASA) and French (Centre National d'Etudes Spatiales/CNES) CALIPSO satellite, found that wildfire smoke remains in the boundary layer. It did not observe smoke aloft in a sampling of the CALIPSO global record, except in rare cases far from sources, after other atmospheric processes have had time to lift the smoke to higher elevations [*Labonne et al.*, 2007].

[4] The combination of MISR and CALIOP sampling and sensitivity differences may account for these seemingly disparate, qualitative conclusions about the frequency with which smoke is injected above the ABL. CALIOP is part of the A-Train constellation, having a dayside equator crossing at about 1:30 PM local time, and a field-of-view, before averaging, of 100 m [*Winker et al.*, 2004]. The MISR dayside equator crossing is at about 10:30 AM local time (about an hour later, local time, over most longitudes of Alaska), and its swath is nearly a factor of 4×10^3 wider. Over the 16-day ground-track repeat cycle of both satellites, the lidar samples less than 0.2% of the total surface area of the planet ($<9.3 \times 10^5$ km^2), including day and night, ocean, land, and polar regions. During the same period, MISR views the equivalent of the entire Earth surface about 3.5 times ($\sim 1.8 \times 10^9$ km^2) on the dayside, where it observes reflected visible light. So, ignoring spatial coverage pattern biases that affect primarily the narrow-swath lidar instrument, and diurnal variations in fire intensity that favor the early afternoon CALIPSO over the late morning Terra and especially over the late night CALIPSO observing times, MISR is nearly 4,000 times more likely to observe buoyant plume cores than CALIOP.

[5] The typical smoke plume core is larger than 100 m in the cross-track direction, which increases the probability, compared to MISR, that CALIOP will see some part of it. One way to estimate this factor is to compare the spatial sampling of the two instruments for a pair of adjacent orbits. Assuming a cross-track, near-source plume extent of 10 km, for example, and taking the inter-orbit spacing as 2000 km in mid-low latitudes, MISR will sample about 400/2000, whereas CALIOP will capture approximately 10/2000 of the inter-orbit region. This yields $\sim$40 as a rough estimate of the increased likelihood MISR will observe a typical smoke plume near its source. For larger plumes, the extent may be $\sim$40 km, which would increase the CALIOP detection probability correspondingly.

[6] Several subtleties must be considered. Near sources, smoke plumes are often only a few kilometers in width, and are not necessarily oriented cross-track. So, for example, if CALIOP happens to view just a few hundred meters upwind of a source, it may not see ABL smoke, and is unlikely to see any smoke injected to higher elevations. Although 10 km

[1] Jet Propulsion Laboratory, California Institute of Technology, Pasadena, California, USA.
[2] Now at NASA Goddard Space Flight Center, Greenbelt, Maryland, USA.
[3] Columbus Technologies and Services, Inc., Pasadena, California, USA.
[4] School of Engineering and Applied Sciences, Harvard University, Cambridge, Massachusetts, USA.

0094-8276/08/2007GL032165$05.00

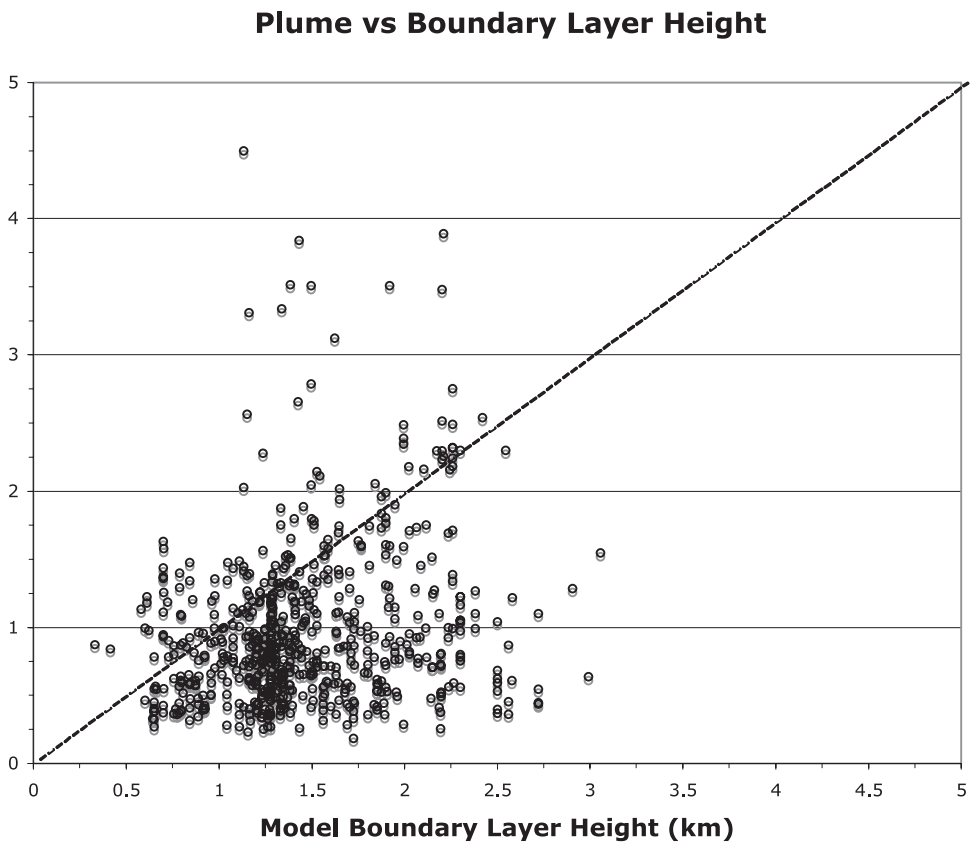

Figure 1. MISR plume vs. model-derived boundary layer heights above the terrain, for 664 plumes in the Alaska-Yukon region, summer 2004. (GEOS-4 boundary layer height is referenced to the terrain; MISR standard product plume heights are reported above the geoid and are corrected here to account for terrain elevation.)

may be a good representative near-source plume length scale, it may need to be divided by a factor of between 2 and 4 to account for directionality and finite width. Also, if CALIOP views a plume far from the source, it would be difficult to assess whether any smoke observed above the ABL had been lofted by initial plume buoyancy or by the subsequent action of other dynamical processes. Provided the location of the CALIOP observation relative to the source is known, e.g., from an imager such as the MODerate resolution Imaging Spectroradiometer (MODIS), 20 to 50 km is probably an appropriate distance to use for proximity, so this does not reduce the coverage estimate further. A third consideration is that CALIOP observes *the same* 0.2% of Earth's surface in every 16-day orbit cycle. The effect of this lidar sampling bias depends on the locations and plume extents for actual fires, which vary on many time scales. Over the 16-day cycle, the grid of orbits has a spacing of about 170 km near the equator, diminishing toward the poles, so all major fire regions globally receive some coverage, though individual events that fall between the orbit tracks will be systematically missed. In summary, MISR is between about 40 and a few hundred times more likely to observe some part of a typical buoyant fire plume core than CALIOP.

[7] On the other hand, the active lidar sensor can measure layer heights of optically very thin aerosol (aerosol optical thickness (AOT) ~0.02, D. Winker, personal communication, 2007), whereas the MISR stereo height technique relies on identifying aerosol or cloud contrast features in multiple, angular views, having AOT of at least a few tenths. Since smaller fires deposit all their aerosol in the ABL, and even the most energetic fires leave some smoke there, CALIOP is much more likely to detect horizontally extensive, but optically thin, boundary layer smoke that the MISR Stereo Height algorithm misses. As such, the MISR and CALIOP measurements are essentially complementary.

[8] We take an initial step toward assessing the contribution wildfires make to above-boundary-layer smoke by calculating the distribution of differences between aerosol source plume height derived from MISR, and ABL height obtained from the Goddard Earth Observing System Model – Version 4 (GEOS-4) [*Bloom et al.*, 2005]. Although the standard MISR product reports elevation above the geoid of the reflecting layer (the level of highest spatial contrast, which may be at the surface, cloud top, or plume top), this product does not classify the results as smoke, dust, water cloud, topography, etc. Early efforts at locating smoke plumes automatically and extracting their heights from the MISR data were made by *Mazzoni et al.* [2007]. In the current analysis, smoke plumes were identified by first using the MODIS MOD-14 fire pixels [*Justice et al.*, 2002; L. Giglio, MODIS Collection 4 Active Fire Product User's Guide, Version 2.0, May 2005, available at http://modis-fire.umd.edu/] to find candidate plume locations in the MISR field-of-view, and then visually inspecting the MISR images to determine where smoke plumes were apparent in the data. Plume shapes and wind directions were digitized manually with the help of an interactive analysis

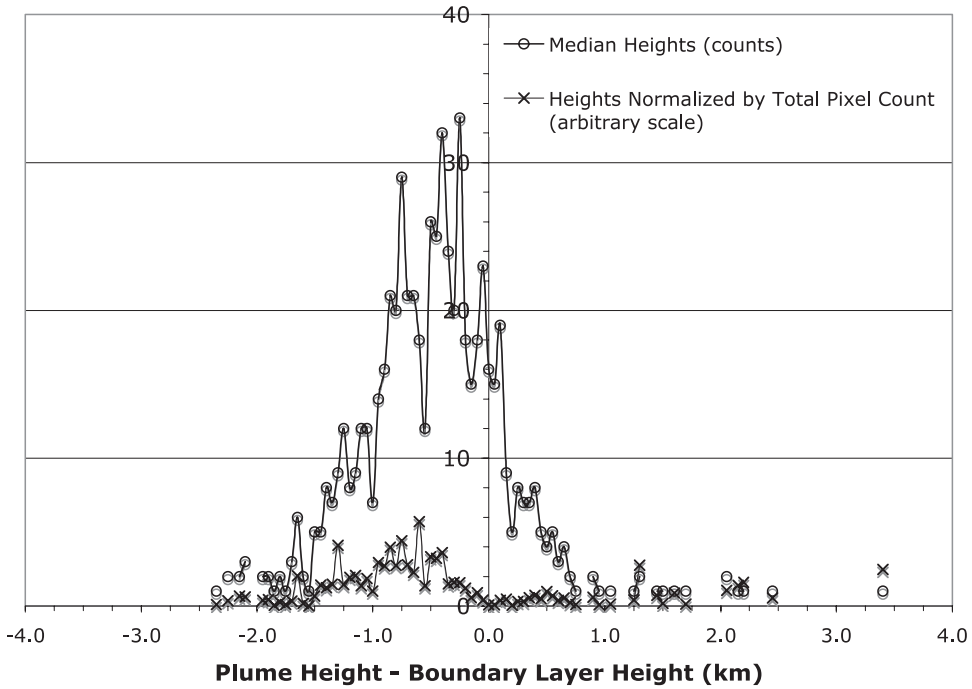

Figure 2. Histograms of plume elevation relative to the nominal ABL, both by plume count and by fraction of total plume area, for 664 plumes in the Alaska-Yukon region, summer 2004. The Normalized Heights were calculated as a count of all pixels from all plumes that fell in a given height difference bin, divided by the total number of pixels from all plumes.

tool. Wind-corrected height above the geoid was calculated to approximately ±200 m accuracy by stereo-matching images from MISR's nadir camera with images from six of MISR's oblique-viewing cameras (all but the 70° views).

[9] The plume height measurement approach adopted here represents a refinement, in several respects, of that developed for the MISR Standard Stereo Height product by *Moroney et al.* [2002] and *Muller et al.* [2002]: (1) Plume occurrence, extent, and wind direction are verified by visual inspection. (2) Taking advantage of the visual inspection step, wind speed and plume height are derived simultaneously and at the same high spatial resolution of 275 m, rather than retrieving wind direction along with wind speed first, at 70.4 km resolution. Also, thick plumes not identified with MODIS fire pixels due to low fire emissivity or smoke opacity could be captured in this step. (3) Parallaxes from the 46° and 60° forward and aft cameras compared to nadir are included with the 26° comparisons used in the Standard algorithm, yielding up to six estimates of wind and height at each point. (4) Surfaces are fitted to the camera-match correlation matrices to provide sub-pixel disparity estimates, improving vertical resolution. ABL height from the GEOS-4 model was aggregated to a 2° latitude × 2.5° longitude grid, for 55 vertical levels from the surface to 0.01 hPa, at 3-hour intervals, with an uncertainty estimated at ±500 m [*Global Modeling Assimilation Office*, 2004]. The ABL value used here was interpolated to MISR overpass time between the pair of bracketing model results.

[10] We performed an initial search over central Alaska and the Yukon between mid-June and mid-September 2004, coinciding with the INTEX-A field campaign period. We found 664 smoke plumes over an area extending from ~130° to ~170° W longitude, north of ~50° N latitude. A scatter plot of MISR plume vs. model ABL elevations for these events is given in Figure 1; the difference between plume and ABL height (Plume - ABL height) results are presented in Figure 2, and are summarized in Table 1. The total area covered by digitized plumes amounts to about 1.7×10^5 km^2, acquired during 79 MISR orbits.

[11] Based on Figure 1, smoke from a significant fraction of fire events in this data set is injected above the ABL, and in many of these cases, the height difference exceeds the ~0.5 km uncertainty in the heights themselves. When the plume height exceeds about 2 km, there is no apparent correlation between plume and ABL height, suggesting other factors, such as atmospheric stability structure, are also involved.

[12] Figure 2 takes a more detailed look at Plume - ABL height, where it is assessed in two ways: (1) Normalized Heights were calculated as a count of all pixels from all plumes that fell in a given height difference bin, normalized by the total number of pixels from all plumes. (2) Median Heights were obtained separately for each individual plume event, where the elevation was determined by fitting a plane through the heights of all pixels in that plume, but discarding heights more than 1.5 standard deviations from the plane, and finding the median of the remaining heights. The more conservative median plane estimate de-emphasizes the larger plumes, and at the same time, helps remove possible contributions from convective overshoot or isolated pyro-

Table 1. Summary of 664 Alaska-Yukon Smoke Plume Statistics for Summer 2004

	All Smoke Pixel Heights by Area	Median Plane Heights
[Plume-ABL] Height > 0	21.4%	20.4%
[Plume-ABL] Height > 0.5 km	17.6%	5.4%

cumulus and other cloud that might appear as above-boundary-layer smoke. The extent of each plume itself is defined visually, and for the purpose of this analysis, covers the coherent smoke cloud emanating from the apparent source, but not any diffuse aerosol in the surroundings. Obvious clouds were also eliminated from the height maps, based on visual inspection of texture, cloud shadows, etc.

[13] Calculated either by normalized area or by individual event, the peak of the distribution is −0.25 km, essentially within the ABL. As expected, the median plane method produced fewer above-boundary-layer counts. But from the population under study, about a fifth of plumes overall appear to contribute smoke directly to the free troposphere. In this case, the above-ABL smoke could be especially important for aerosol transport to high latitudes, including snow and ice-covered surfaces. Also given in Table 1 is the percent of counts for which the Plume - ABL height difference is >0.5 km, which captures cases having height differences that exceed the magnitude of expected uncertainties in the plume and ABL heights. Between 5% and 18% of cases meet this criterion (at least 36, and possibly as many as 117 plumes), and the events that do inject smoke to these heights are generally the larger ones, as expected, and as indicated by the difference between area-weighted and median-count values. Similar statistics appear in a preliminary analysis of fire plumes covering North America during 2002.

[14] However, the data presented here do not provide a precise measure of plume "size." There is only a very weak correlation between plume area, defined as described above, and (Plume - ABL height), to which ambiguities in the way plume area is defined contribute. The correlation between MODIS fire radiant energy flux and (Plume-ABL height) is also weak, most likely caused by a combination of varying fire emissivity and varying smoke opacity above the fire pixels, both of which affect the satellite signal, along with the influence of the atmospheric stability structure on smoke plume elevation itself [e.g., *Kahn et al.*, 2007]. None of these effects is included in the present analysis. So estimating the *amount* of smoke injected above the ABL will require additional steps; these might include using aerosol optical depths from MISR and MODIS in the plume as well as the surroundings, and MISR source plume height, along with CALIOP aerosol vertical distribution (which in general is obtained some distance from the fire source), to constrain a regional aerosol transport model. As the data analyzed here cover only a single region, others areas and seasons must be studied as well, to obtain a global picture. These extensions are beyond the scope of the current note, but the subject is ripe for further study.

[15] **Acknowledgments.** We thank our colleagues on the Jet Propulsion Laboratory's MISR instrument team and at the NASA Langley Research Center's Atmospheric Sciences Data Center for their roles in producing the MISR data sets, and François-Marie Bréon for sharing his insights on CALIPSO sampling. This research is supported in part by NASA's Climate and Radiation Research and Analysis Program under H. Maring, NASA's Atmospheric Composition Program under P. DeCola, NASA's Applied Sciences Program under L. Friedl, the EOS-MISR instrument project, and the EPA STAR program on Fire, Climate, and Air Quality, under subcontract with Harvard University. F.-Y. Leung and J. A. Logan were supported by a grant from the National Science Foundation, ATM-0554804 to Harvard University. This work was performed primarily at the Jet Propulsion Laboratory, California Institute of Technology, under contract with NASA.

References

Bloom, S., et al. (2005), Documentation and validation of the Goddard Earth Observing System (GEOS) Data Assimilation System, version 4, *Tech. Rep. Ser. Global Modeling Data Assimilation NASA/TM 2005-104606*, *vol. 26*, NASA, Greenbelt, Md.

Colarco, P. R., M. R. Schoeberl, B. G. Doddridge, L. T. Marufu, O. Torres, and E. J. Welton (2004), Transport of smoke from Canadian forest fires to the surface near Washington, D. C.: Injection height, entrainment, and optical properties, *J. Geophys. Res.*, *109*, D06203, doi:10.1029/2003JD004248.

Fromm, M. D., and R. Servranckx (2003), Transport of forest fire smoke above the tropopause by supercell convection, *Geophys. Res. Lett.*, *30*(10), 1542, doi:10.1029/2002GL016820.

Ginoux, P., M. Chin, I. Tegen, J. Prospero, B. Holben, O. Dubovik, and S.-J. Lin (2001), Sources and distributions of dust aerosols simulated with the GOCART model, *J. Geophys. Res.*, *106*, 20,255–20,273.

Global Modeling and Assimilation Office (2004), File specification for GEOS-DAS gridded output, version 5.3, *GMAO-1001v5.3*, NASA, Greenbelt, Md.

Justice, C. O., L. Giglio, S. Koronitzi, J. Owens, J. Morisette, D. Roy, J. Descloitres, S. Alleaume, F. Petitcolin, and Y. Kaufman (2002), The MODIS fire products, *Remote Sens. Environ.*, *83*, 244–262.

Kahn, R. A., W.-H. Li, C. Moroney, D. J. Diner, J. V. Martonchik, and E. Fishbein (2007), Aerosol source plume physical characteristics from space-based multiangle imaging, *J. Geophys. Res.*, *112*, D11205, doi:10.1029/2006JD007647.

Labonne, M., F.-M. Bréon, and F. Chevallier (2007), Injection height of biomass burning aerosols as seen from a spaceborne lidar, *Geophys. Res. Lett.*, *34*, L11806, doi:10.1029/2007GL029311.

Mazzoni, D., J. A. Logan, D. Diner, R. Kahn, L. Tong, and Q. Li (2007), A data-mining approach to associating MISR smoke plume heights with MODIS fire measurements, *Remote Sens. Environ.*, *107*, 138–148.

Moroney, C., R. Davies, and J.-P. Muller (2002), MISR stereoscopic image matchers: Techniques and results, *IEEE Trans. Geosci. Remote Sens.*, *40*, 1547–1559.

Muller, J.-P., A. Mandanayake, C. Moroney, R. Davies, D. J. Diner, and S. Paradise (2002), Operational retrieval of cloud-top heights using MISR data, *IEEE Trans. Geosci. Remote Sens.*, *40*, 1532–1546.

Westphal, D. L., and O. B. Toon (1991), Simulations of microphysical, radiative, and dynamical processes in a continental-scale forest fire smoke plume, *J. Geophys. Res.*, *96*, 22,379–22,400.

Winker, D. M., W. H. Hunt, and C. A. Hostetler (2004), Status and performance of the CALIOP Lidar, *Proc. SPIE*, *5575*, 8–15.

Y. Chen, D. J. Diner, and Q. Li, Jet Propulsion Laboratory, California Institute of Technology, 4800 Oak Grove Drive, Pasadena, CA 91109, USA.

R. A. Kahn, NASA Goddard Space Flight Center, Code 613.2, Greenbelt, MD 20771, USA. (ralph.kahn@jpl.nasa.gov)

F.-Y. Leung and J. A. Logan, School of Engineering and Applied Sciences, Harvard University, Cambridge, MA 02138, USA.

D. L. Nelson, Columbus Technologies and Services, Inc., 225 S. Lake Avenue, Suite 1010, Pasadena, CA 91101, USA.